Authors responses (ACs) to RC2 Comments on amt-2021-339

We thank the reviewer for their careful reading of our manuscript and their comments. Each reviewer comment is reproduced in *italics* below, followed by our response in blue text.

RC2: 'Comment on amt-2021-339', Anonymous Referee #2, 20 Dec 2021

The manuscript shows results of the Ny-Ålesund Ozone in the Mesosphere Instrument, NAOMI, at the UK research station in Ny-Ålesund on Spitsbergen during the period August 2017 to March 2020.

The results are seasonally binned and compared to simultaneous observations of the SABER instrument onboard the TIMED satellite.

The differences between NAOMI and SABER are then also compared to the internal differences of the two SABER channels at 9.6 and 1.7 µm.

The paper presents ozone measurements at 11.072 GHz following the instrumental concept of the MOSAIC instruments developed during the last 13 years. This way the paper does not present unique or novel work. It rather builds on and develops previous work by for instance Rogers from 2009 and 2012 in observing ozone in the mesosphere and lower thermosphere, a region hard to explore by ground-based instruments.

However, in this paper a more complex data analysis with the help of ARTS is performed instead of Roger's two parameter model. In this respect the paper presents a novel approach.

The goal of the paper is to contribute to a better understanding of the vertical distribution of Ozone in the Northern polar region. Given the already existing network of similar instruments and their low costs this paper might even encourage to set up new instruments at different places in order to increase the network.

Major comments

The binning of data is sometimes crucial. While SABER has a 60-day period looking North, the NAOMI data are binned over 90 days. What is the justification for that? And how does this affect the averaged result of the NAOMI data?

The reviewer questions the justification for binning NAOMI data over 90-day periods (i.e., 15 December–15 March for 'winter', 15 April–15 July for 'summer', and 15 August–15 November for 'autumn') when SABER has 60-day periods viewing north. In fact, NAOMI and SABER observations *within* each nominal 90-day period are carefully selected to meet the solar zenith angle criteria and additionally, for SABER, overlap with the NAOMI observing location. Figure AC-1 shows that the selected NAOMI and SABER observation times, in this case for 2017–18 winter night-time conditions, overlap and are well matched. The overlap period is indeed rather shorter than 90 days, in this case from 29 December 2017 to 16 February 2018. This period is well within the 60-day northward viewing SABER yaw period. As shown in Figure AC-2, SABER provides uniform coverage between latitudes 77 °N and 84 °N during this period and the mean observation latitude at 90 km of 81.4 °N is

within a degree of that for NAOMI (82.3 °N). The corresponding observation time and latitude plots for all nine scenarios (Appendix ACA1 – Figures ACA1-1–9 and Appendix ACA2 – Figures ACA2-1–9) show similar levels of overlap between the selected NAOMI and SABER datasets. Therefore, we consider the method used to select, bin, and average overlapping NAOMI and SABER data is justified. We do note, however, that the description of the binning method could be clearer. The actual start and end dates for the season in each case will be stated in the Figure and Table captions. As well as the additional text given in our response to RC1's first minor comment, we will also add the following to line 125, after the sentence ending '… meteorological definitions of the seasons.'

'In all cases the averaged NAOMI measurements occurred within 3 hours of the selected SABER observation times (see section 2.2), as well as meeting the SZA criteria at 90 km.'

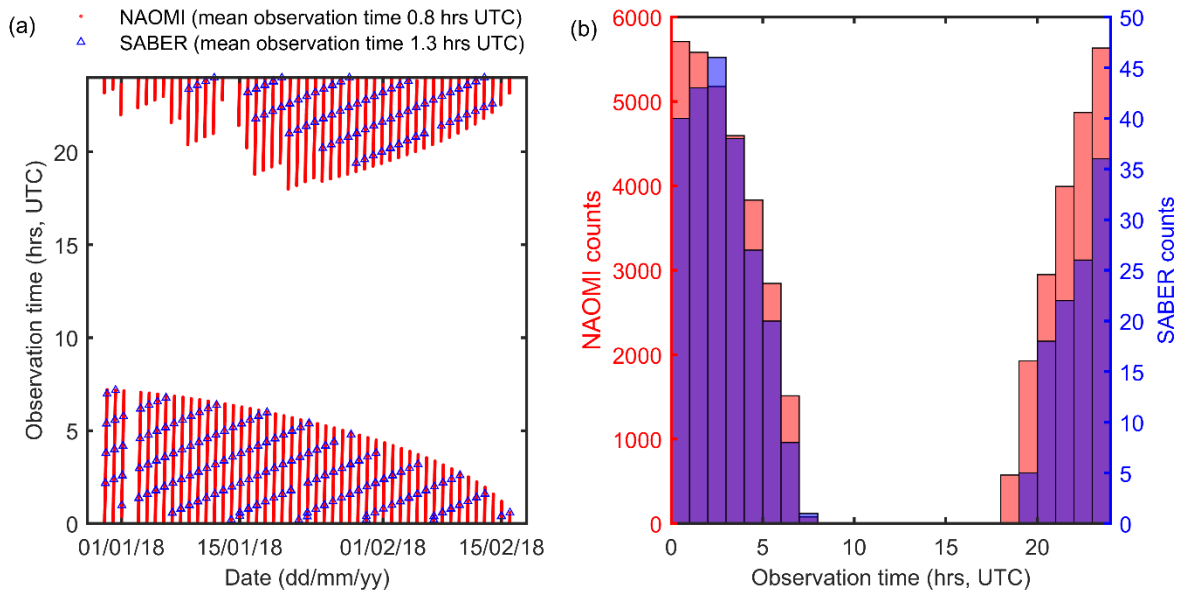

Figure AC1: Observation times for NAOMI and SABER observations during 2017–18 winter night-time (29 December 2017 – 16 February 2018, SZA at altitude 90 km > 110°) conditions: (**a**) time series and **(b)** histograms of NAOMI and SABER observation times.

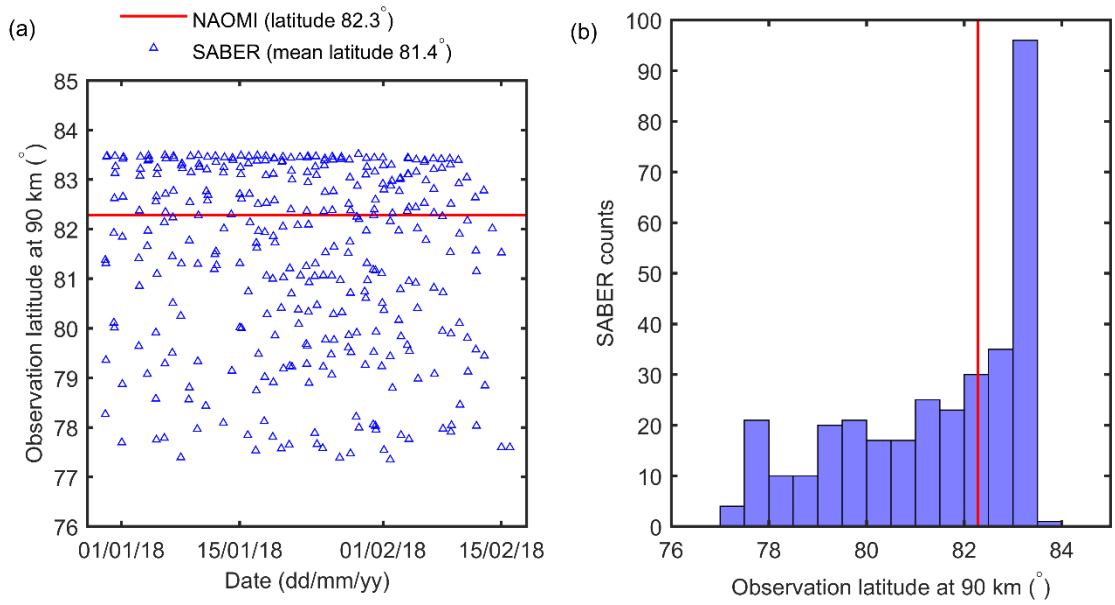

Figure AC2: Latitudes at altitude 90 km for NAOMI and SABER observations during 2017–18 winter night-time (29 December 2017 – 16 February 2018, SZA at altitude 90 km > 110°) conditions: **(a)** time series of observation latitudes and **(b)** histogram of SABER observation latitudes compared with NAOMI observation latitude (red vertical line).

The autumn 2019 data are not presented as the NAOMI time series only includes 40 days of data. But if these data have simultaneous co-located data from SABER this would still be interesting to see. A larger error bar due to a poorer SNR is not necessarily a good reason NOT to show the data, unless the NAOMI data are completely unreasonable.

Figure 8 and **Figure 9** have been amended to include the autumn 2019 twilight data. The sentences starting on line 125 will be changed to the following.

'NAOMI data were not recorded from 26 September to 14 November 2019 due to a temporary instrument fault. Averaging a smaller subset of valid observations between 29 August and 25 September 2019 produces an O_3 spectrum with poorer signal-to-noise compared to a complete autumn dataset but is included in the analysis for completeness.'

The discussion of Figure 8 on lines 270–273 will be revised as follows to include the 2019 autumn twilight data. The SZA data for 2019 autumn twilight is taken from Figure AC3.

'For the two years 2017 and 2018, where the most complete autumn twilight measurements are available, the NAOMI secondary maximum VMRs are 47% and 59% of the SABER peak values respectively. The largest differences are at altitudes above 88 km, in the secondary O_3 layer, whereas below 88 km the NAOMI and SABER profiles agree to within the measurement uncertainties. The 2019 autumn twilight profiles show even larger differences with no secondary O_3 peak in the NAOMI profile. The differences for the 2019 dataset may be due to the shorter period (29 August – 25 September) of NAOMI measurements compared to the previous two years (2 September – 3 November 2017 and 31 August – 1 November 2018). As well as lower signal-to-noise in the integrated NAOMI spectra affecting the O_3 retrieval, during the earlier autumn 2019 period more of the NAOMI observations would have occurred in sunlit conditions (mean SZA 88.6° at 90 km) compared to SABER (mean SZA 90.3° at 90 km), potentially affecting mesospheric O_3 abundances.'

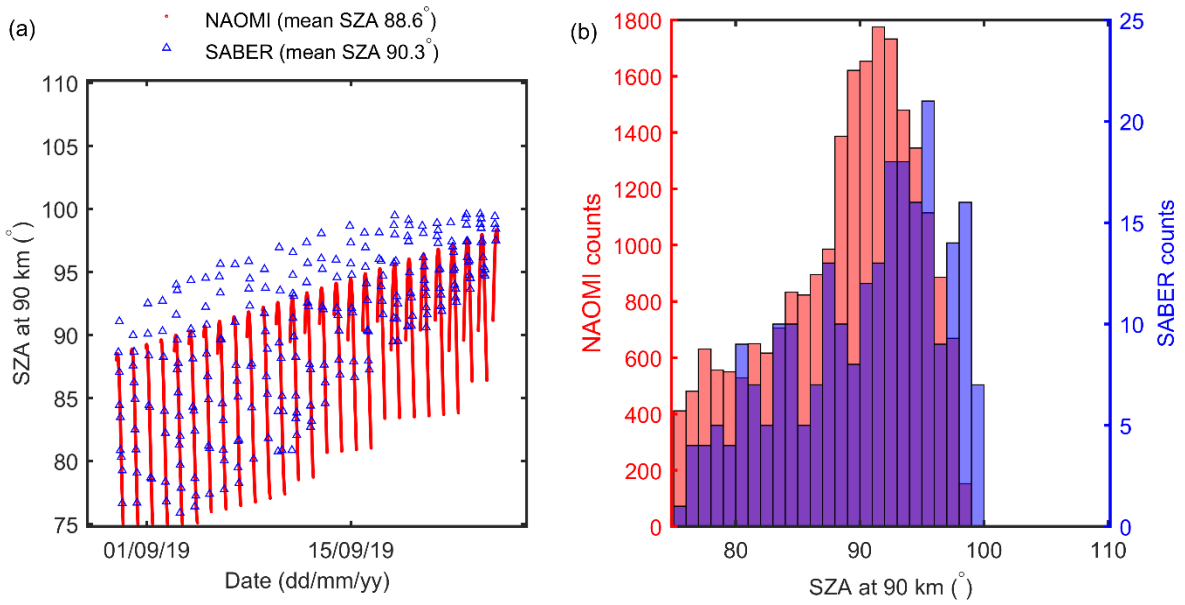

Figure AC3: Solar zenith angles (SZAs) at altitude 90 km for NAOMI and SABER observations during 2019 autumn twilight (29 August – 25 September 2019, 75° ≤ SZA at altitude 90 km ≤ 110°) conditions: (**a**) time series and **(b)** histograms of NAOMI and SABER SZAs.

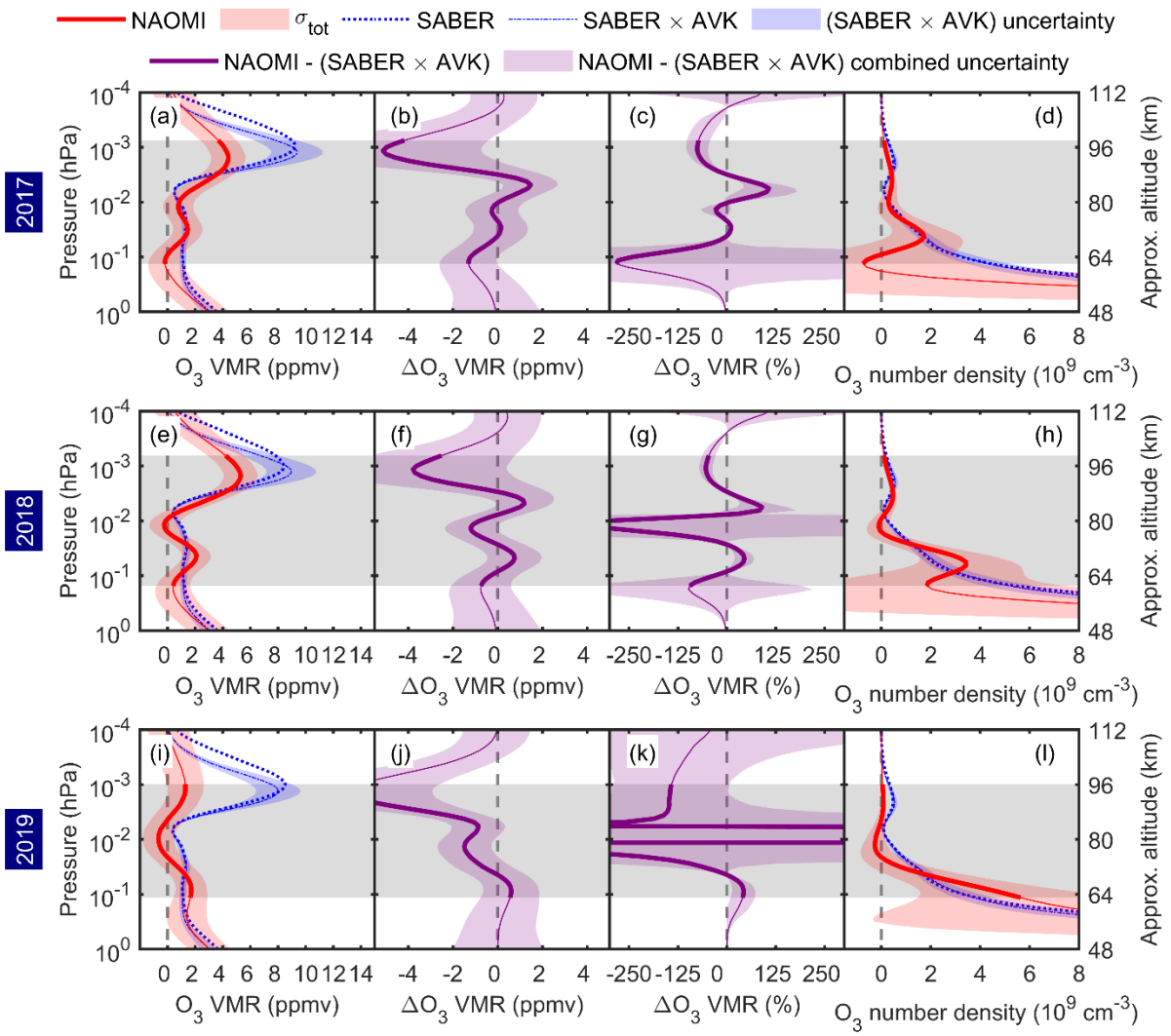

Figure 8: Mean ozone vertical profiles from NAOMI and SABER 9.6 μm observations during autumn twilight (within 15 September–15 November, 75° ≤ SZA at altitude 90 km ≤ 110°) conditions in 2017 (**a**–**d**), 2018 (**e**–**h**), and 2019 (**i**–**l**). The second and third columns give the absolute and relative (%) differences (NAOMI minus SABER 9.6 μm). The red, blue, and purple shading are the estimated uncertainties of the plotted parameters. The grey shaded regions and thicker sections of the plotted curves indicate the pressure and altitude ranges where MR ≥ 0.8.

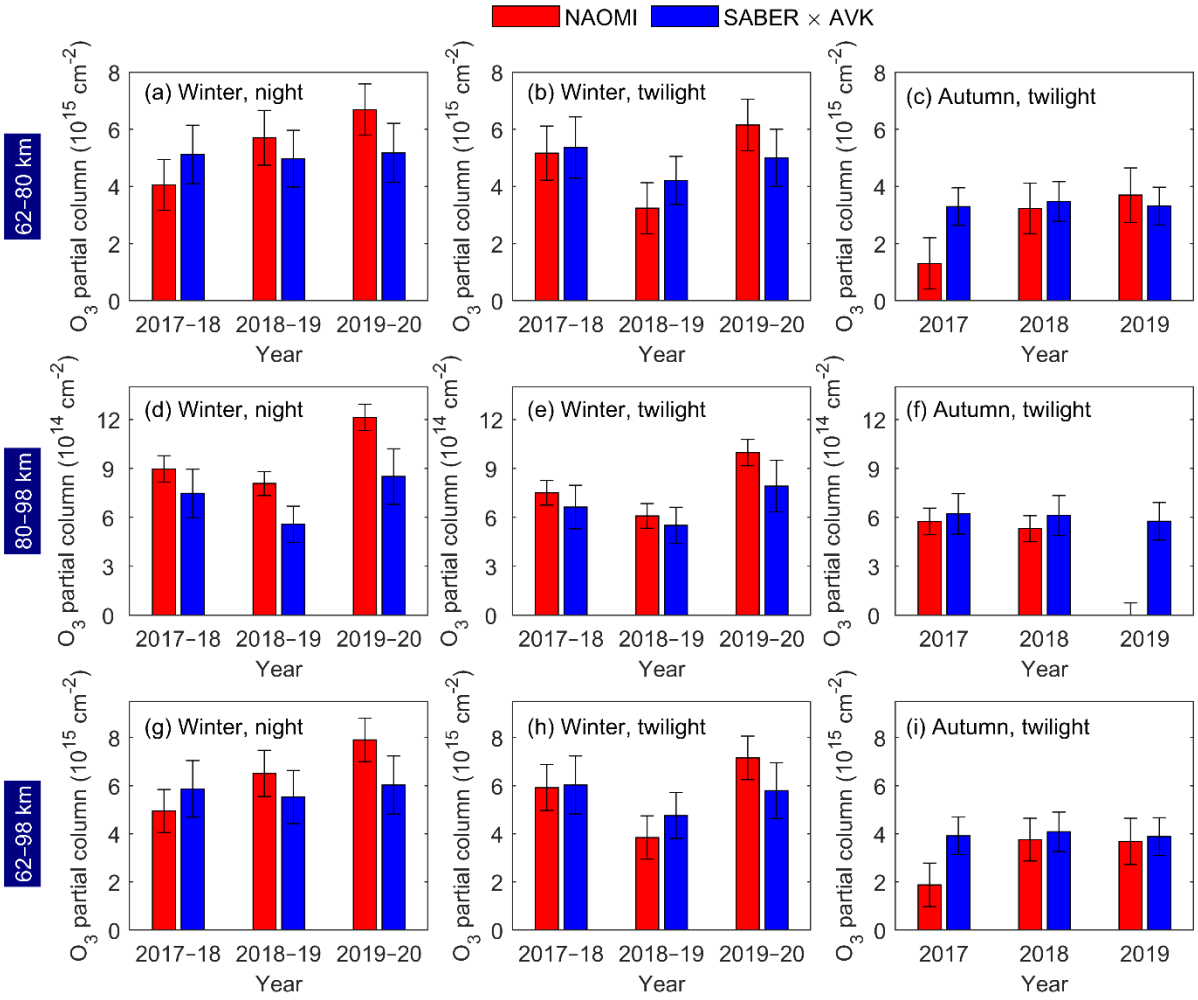

Figure 9: Mean ozone partial columns at 62–80 km (**a**–**c**), 80–98 km (**d**–**f**), and 62–98 km (**g**–**i**) from NAOMI and SABER 9.6 µm observations during night-time winter (left column), winter twilight (centre column), and autumn twilight (right column) conditions in 2017–20. The error bars are the estimated uncertainties of the plotted parameters. Note that the partial column scales for the upper (a–c), middle (d–f), and lower (g–i) panel plots differ.

The choice of the grid points for both WACCM-D and MERRA-2 are chosen such that they are close to the instrument. The tangent point of the measurement at 90 km altitude, however, is roughly 470 km towards North-West. The authors do not expect a significant variation in the results due to changes in the observation conditions over such a large area?

We do not expect a significant variation in the results due to changes in observation conditions between the instrument location on the ground and the upper mesosphere at 90 km altitude. Using MERRA-2 water vapour VMR and temperature profiles below 10^{-2} hPa from the grid point closest to Ny-Ålesund is appropriate as it allows the forward model to calculate background microwave attenuation which will be highest in the troposphere (altitudes 0–10 km) within ~50 km of NAOMI. As we point out in our response to the reviewer's next comment, microwave transmission at 11.072 GHz is relatively insensitive to changes in humidity and temperature in different Arctic locations or seasons and has a small effect on the NAOMI O_3 measurements. Similarly, we use SABER temperatures between 10^{-2} hPa and 10^{-4} hPa within the box centred on the 90 km observation altitude shown in Figure 1. As stated in lines 155–157, this selection provides more realistic mesospheric temperature profiles than using WACCM-D averages. Finally, our error analysis (Figure 5

and lines 239–248) estimates contributions to uncertainties in the O_3 retrieval which includes the WACCM-D O_3 VMR a priori above 10^{-2} hPa.

Given the fact that Spitsbergen is an island, the surrounding water might have an effect on at least the tropospheric (observation) conditions with respect to for instance tropospheric water vapor and its high variability? At an elevation angle of 11° I would expect quite some variability in observation conditions and thus in data quality. Has there been any discrimination of data due to 'bad weather' conditions? When the signal of a three-months period adds up to 60 mK I would appreciate some more details on the radiative transfer and how a varying tropospheric water vapour content affects the measurements and the averaging process.

We have previously shown (Figure 5 in Newnham et al., 2019*) that different seasonal meteorology at various polar locations will have little impact on microwave observations such as those made by NAOMI. Atmospheric transmittance with elevation angle 8° is calculated to vary between 0.85 and 0.86 at 11.072 GHz in summer and winter at six different Arctic and Antarctic locations including a relatively mild coastal site (Reykjavik) and an elevated cold, dry location (Pillow Knob, continental Antarctica). Therefore, we do not expect varying tropospheric water vapour content to significantly affect the measurements and averaging process. It is possible that poor weather conditions such as heavy precipitation could affect the microwave measurements and we agree with the reviewer that in future screening the data for such events could improvements data the quality. We will add the following text after line 128.

'Differing seasonal meteorology has been assessed (Newnham et al., 2019) to have little impact on Ku-band microwave observations such as those made by NAOMI in polar conditions, even when viewing the atmosphere at shallow angles such as 11° elevation. Therefore, we do not expect varying tropospheric water vapour content to significantly affect the measurements and averaging process. Heavy precipitation during poor weather conditions could potentially affect the measurements and attenuate the mesospheric O_3 emission signal through microwave absorption and scattering. Future screening for such weather events, and removal of affected microwave data, could yield improvements in the data quality.'

*Newnham, D. A., Clilverd, M. A., Kosch, M., Seppälä, A., and Verronen, P. T.: Simulation study for ground-based Ku-band microwave observations of ozone and hydroxyl in the polar middle atmosphere, Atmos. Meas. Tech., 12, 1375–1392, https://doi.org/10.5194/amt-12-1375-2019, 2019.

The criteria for 'co-location' and 'overlapping' observations of SABER and NAOMI measurements is not entirely clear to me. Are all SABER measurements under twilight conditions (75° < SZA < 110°) during a 60-day period within the area depicted in Fig. 1 binned together and averaged without considering the location or the time of the day? Could the authors elaborate briefly on their choice of binning and whether this binning is acceptable with respect to the rather strong diurnal variation between midday and midnight ozone concentration. During the twilight period the profiles should vary quite a bit. But probably I missed some important facts here.

SABER measurements within the area depicted in Figure 1 are selected and binned into seasonal periods and SZA at altitude 90 km for daytime, twilight, and night-time conditions.

NAOMI measurements occurring within 3 hours of the SABER observation times and meeting the SZA criteria at 90 km are then selected and averaged. Although location and time of day are not explicitly considered, we show in Figures AC4–6 that there is good overlap between the selected NAOMI and SABER locations (latitudes), SZAs, and observation times. Figure AC4 shows that, while SABER observations cover the latitude range 77.3–83.5 °N for 2017 autumn twilight conditions, the mean latitude of 81.1 °N is close to the NAOMI observation at 82.3 °N. Considering SZA, although SABER observations extend to several degrees higher SZA than NAOMI (Figure AC5) the histogram distributions show reasonable overlap and mean SZA differs by just 1.4°. Thirdly, the observation times (Figure AC5) are closely matched with mean UTC of 0.4 hrs for NAOMI and 0.5 hrs for the SABER selection. The corresponding latitude, SZA, and observation time plots for all nine scenarios (Appendix ACA1 – Figures ACA1-1–9, Appendix ACA2 – Figures ACA2-1–9, and Appendix ACA3 – Figures ACA3-1–9) show similarly high levels of overlap between the selected NAOMI and SABER datasets. We therefore consider our selection and binning methodology is valid.

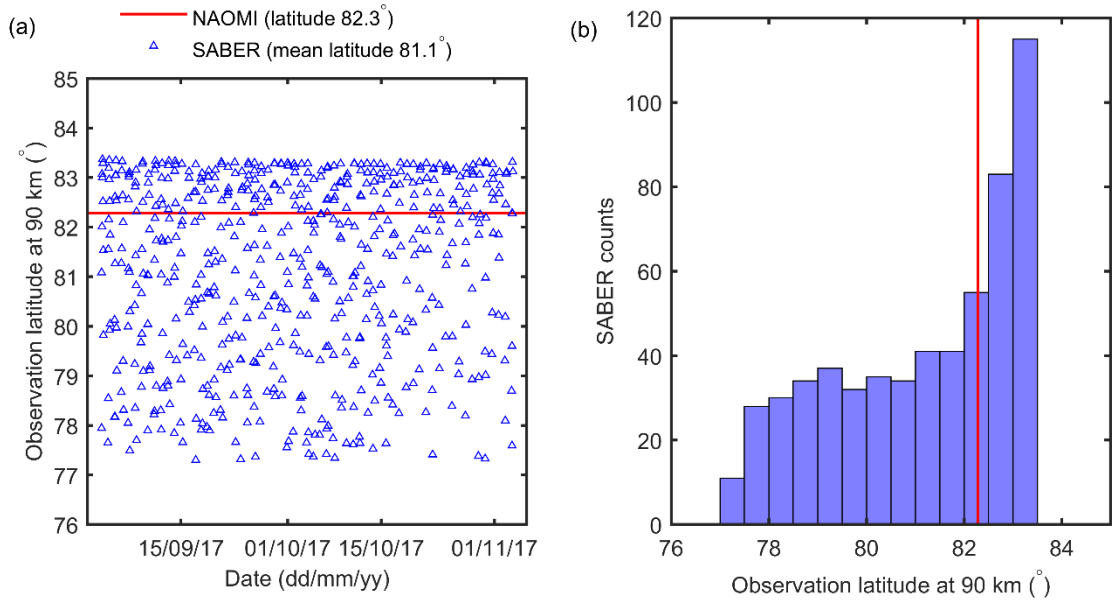

Figure AC4: Latitudes at altitude 90 km for NAOMI and SABER observations during 2017 autumn twilight (2 September – 3 November 2017, 75° ≤ SZA at altitude 90 km ≤ 110°) conditions: (**a**) time series of observation latitudes and **(b)** histogram of SABER observation latitudes compared with NAOMI observation latitude (red vertical line).

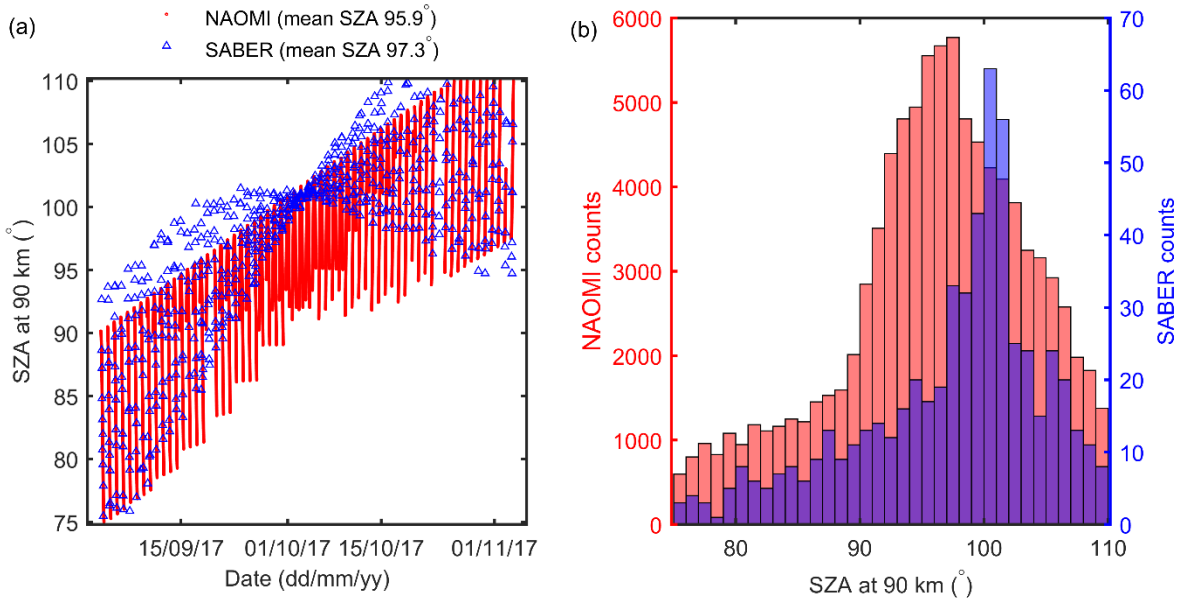

Figure AC5: Solar zenith angles (SZAs) at altitude 90 km for NAOMI and SABER observations during 2017 autumn twilight (2 September – 3 November 2017, 75° ≤ SZA at altitude 90 km ≤ 110°) conditions: (**a**) time series and **(b)** histograms of NAOMI and SABER SZAs.

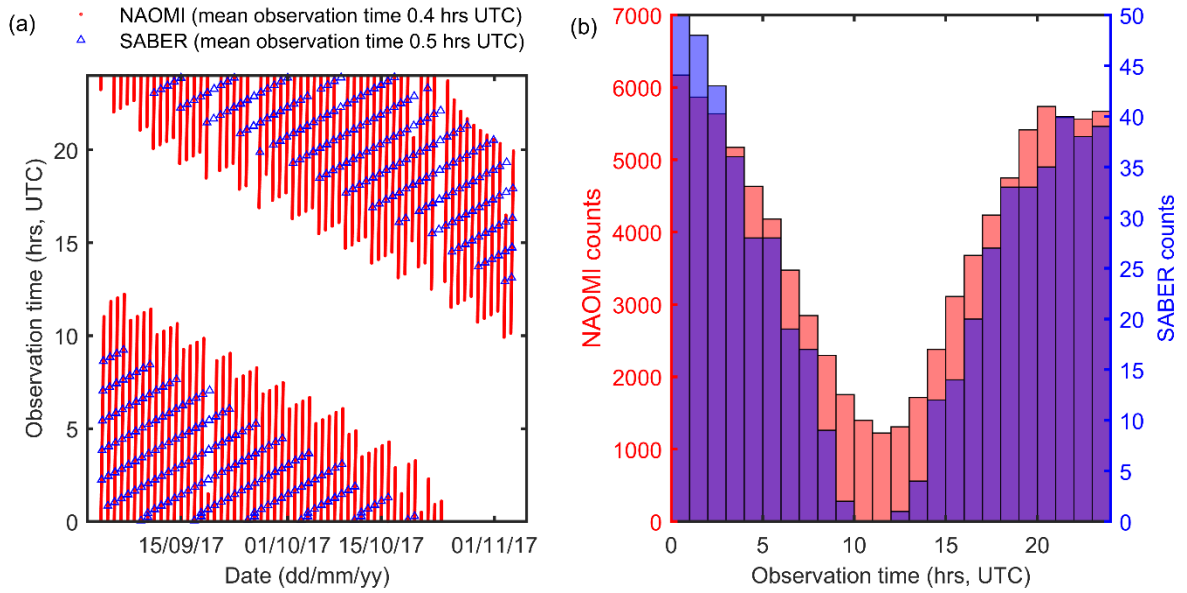

Figure AC6: Observation times for NAOMI and SABER observations during 2017 autumn twilight (2 September – 3 November 2017, 75° ≤ SZA at altitude 90 km ≤ 110°) conditions: (**a**) time series and **(b)** histograms of NAOMI and SABER observation times.

Minor comments

Fig 1: The red line depicting the line of sight of NAOMI is hard to see, even harder so are the red triangles. Would a white or black line be more visible?

Thanks to the reviewer for pointing this out. The red line and symbols in **Figure 1** have been changed to black and the caption updated.

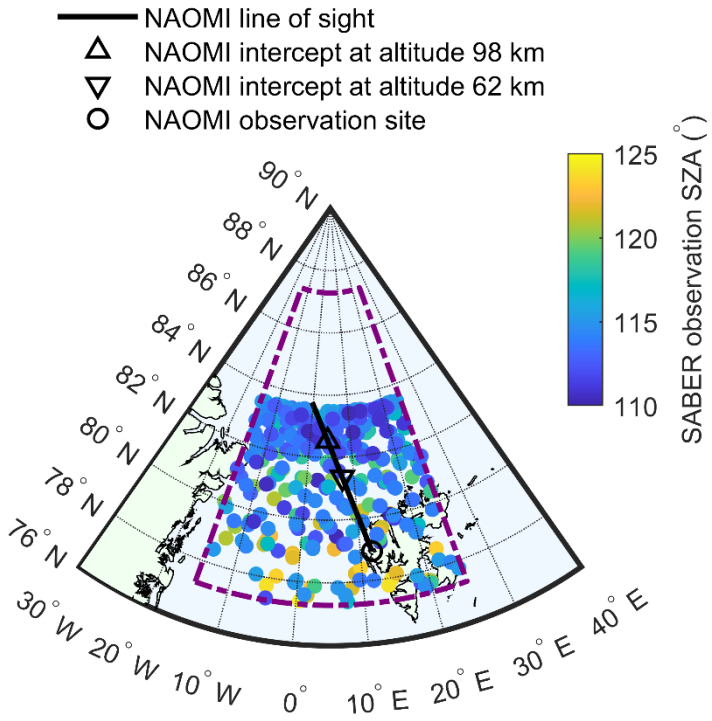

Figure 1: Map of Svalbard and the Arctic region poleward of geographic latitude 76° N and from 30° W to 40° E. The black circle shows the NAOMI ground-based location (78°55'0" N, 11°55'59" E). The black line is the projection of the line-of-sight view of NAOMI at elevation angle 11° and azimuth 345°. The dashed purple box shows the region ±20° longitude and ±5° latitude of the NAOMI intercept at altitude 90 km (82°16'57" N, 5°6'50" E) used for selecting overlapping SABER observations. The filled, coloured circles show the locations and SZAs of SABER observations within the dashed purple box during night-time conditions (SZA at altitude 90 km > 110°) in the 2017–18 winter (29 December 2017 – 16 February 2018).

Fig 6, 7 and 8: in d), h), and l) the uncertainty of the NAOMI O3 number density at lower altitudes is shown as a large area with a completely different shape of the NAOMI profile compared to the SABER profile. A short comment on the different shapes occurring in the plots would be appreciated, especially when this big difference is not reflected in the (binned) column densities for the lower altitudes in Fig. 9.

The following text will be added to section 3.2 (after line 273) commenting on the differences between the NAOMI and SABER number densities at lower altitudes in Figures 6–8.

'The differences between NAOMI and SABER appear more distinct in the higher O_3 number densities below ~80 km. NAOMI number density profiles show a distinct tertiary peak at ~70 km whereas the SABER densities increase more uniformly with decreasing altitude from 78 km to 62 km. However, the differences between NAOMI and SABER largely disappear

when the number densities over 62–80 km are integrated to produce partial columns, suggesting that the limited height resolution (~11–13 km) of the NAOMI retrieval is a significant factor in the profile shape over this 18 km altitude range.'

Citation: https://doi.org/10.5194/amt-2021-339-RC2

Appendix ACA1 – Plots of NAOMI and SABER observation latitudes

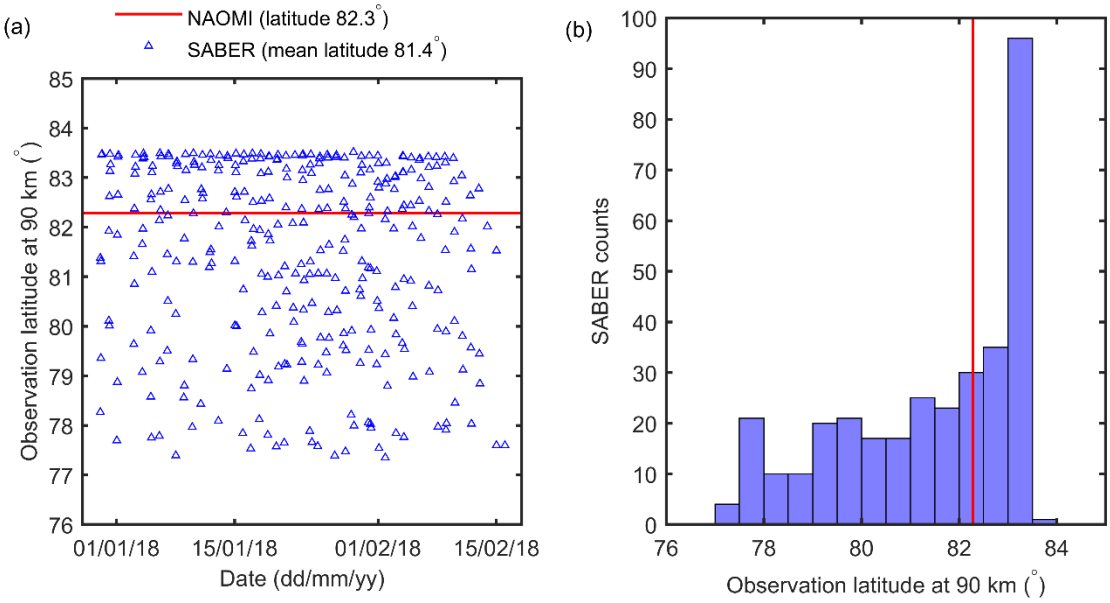

Figure ACA1-1: Latitudes at altitude 90 km for NAOMI and SABER observations during 2017–18 winter night-time (29 December 2017 – 16 February 2018, SZA at altitude 90 km > 110°) conditions: (**a**) time series of observation latitudes and **(b)** histogram of SABER observation latitudes compared with NAOMI observation latitude (red vertical line).

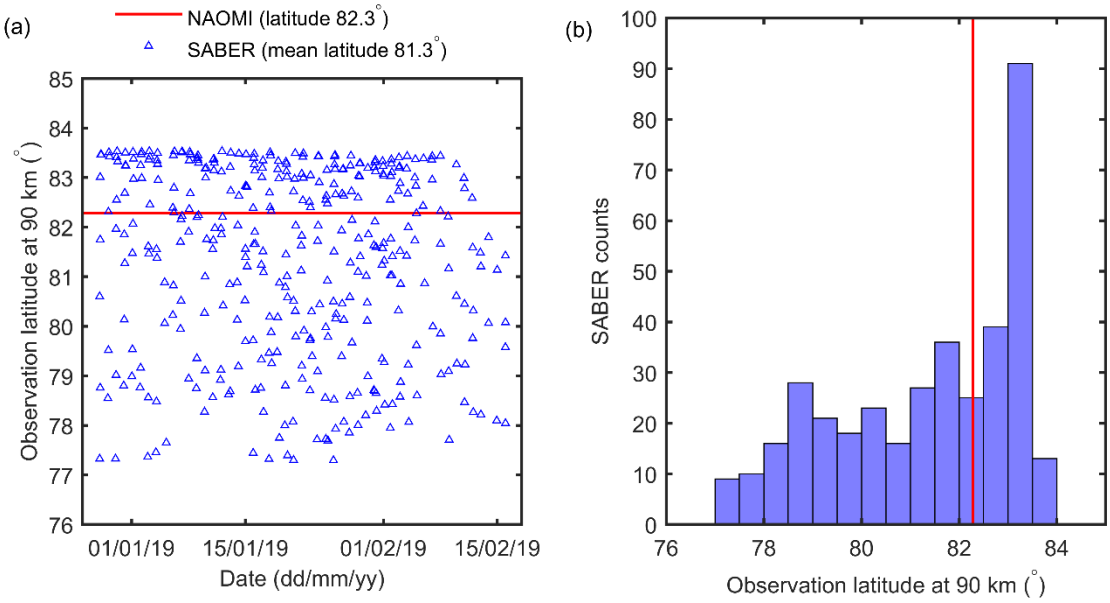

Figure ACA1-2: Latitudes at altitude 90 km for NAOMI and SABER observations during 2018–19 winter night-time (27 December 2018 – 16 February 2019, SZA at altitude 90 km > 110°) conditions: (**a**) time series of observation latitudes and **(b)** histogram of SABER observation latitudes compared with NAOMI observation latitude (red vertical line).

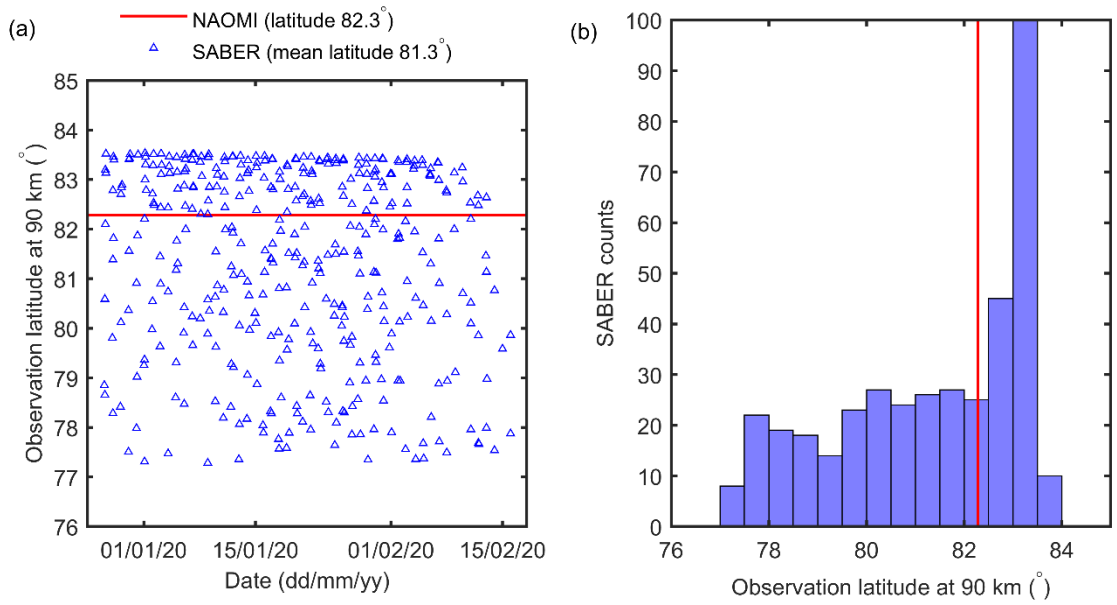

Figure ACA1-3: Latitudes at altitude 90 km for NAOMI and SABER observations during 2019–20 winter night-time (26 December 2019 – 16 February 2020, SZA at altitude 90 km > 110°) conditions: (**a**) time series of observation latitudes and **(b)** histogram of SABER observation latitudes compared with NAOMI observation latitude (red vertical line).

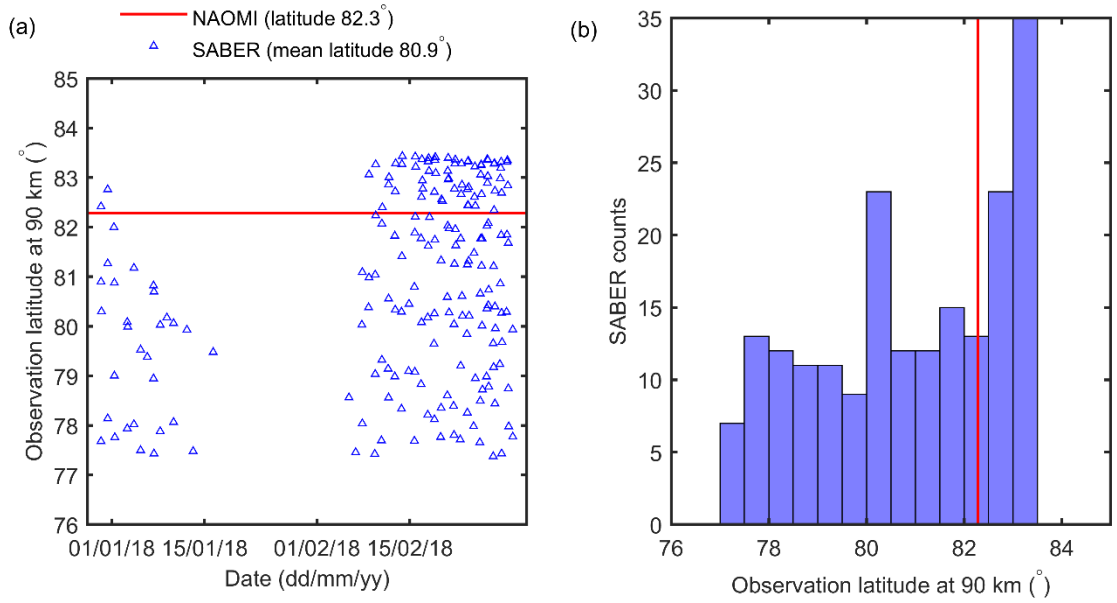

Figure ACA1-4: Latitudes at altitude 90 km for NAOMI and SABER observations during 2017–18 winter twilight (30 December 2017 – 2 March 2018, 75° ≤ SZA at altitude 90 km ≤ 110°) conditions: (**a**) time series of observation latitudes and **(b)** histogram of SABER observation latitudes compared with NAOMI observation latitude (red vertical line).

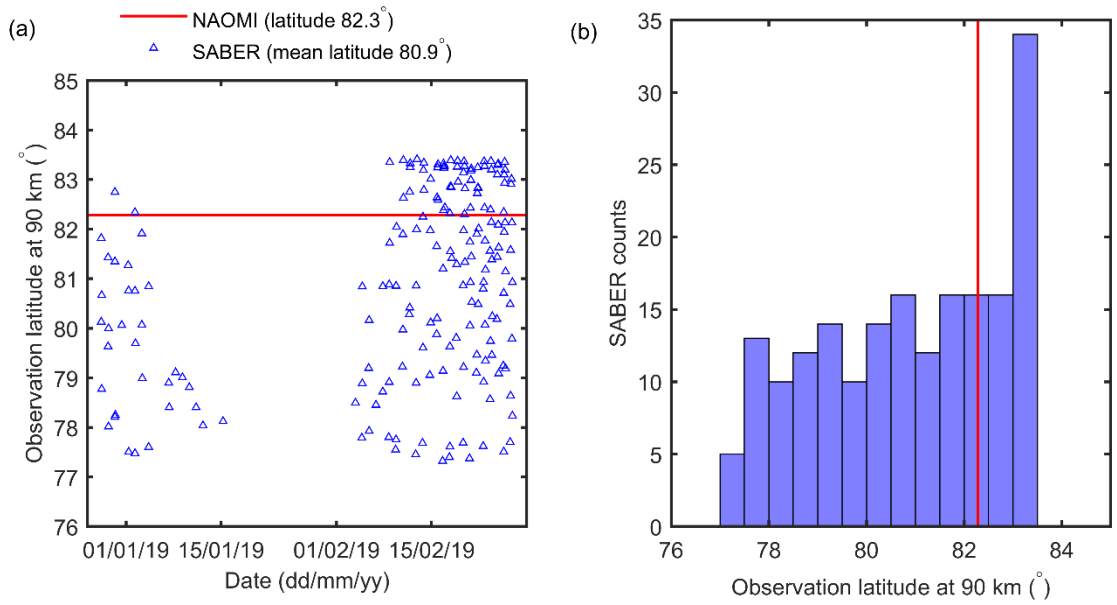

Figure ACA1-5: Latitudes at altitude 90 km for NAOMI and SABER observations during 2018–19 winter twilight (28 December 2018 – 27 February, 75° ≤ SZA at altitude 90 km ≤ 110°) conditions: (**a**) time series of observation latitudes and **(b)** histogram of SABER observation latitudes compared with NAOMI observation latitude (red vertical line).

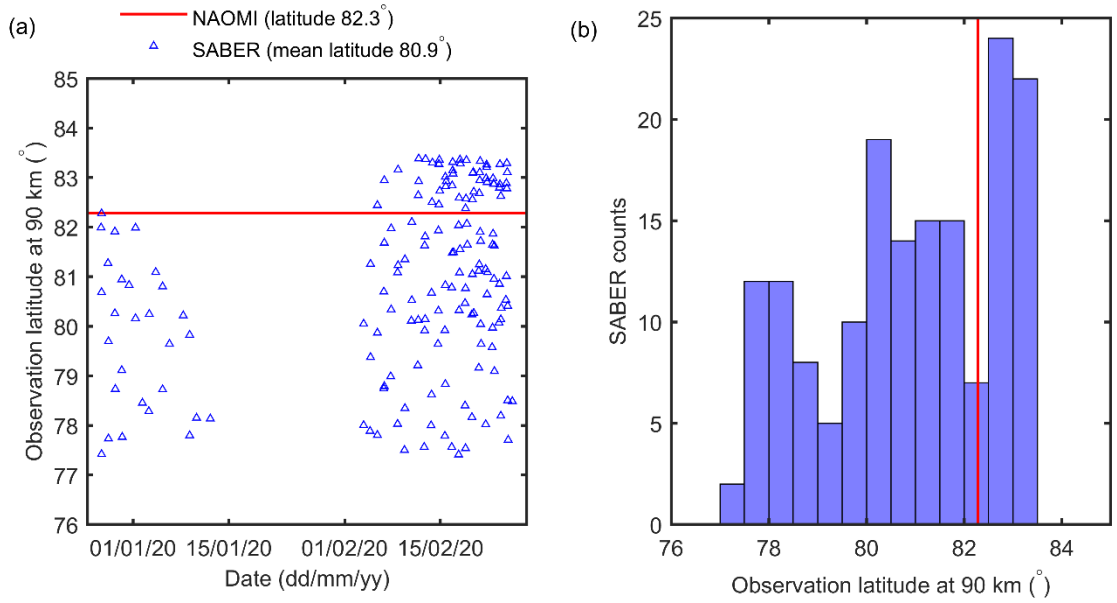

Figure ACA1-6: Latitudes at altitude 90 km for NAOMI and SABER observations during 2019–20 winter twilight (27 December 2019 – 25 February 2020, 75° ≤ SZA at altitude 90 km ≤ 110°) conditions: (**a**) time series of observation latitudes and **(b)** histogram of SABER observation latitudes compared with NAOMI observation latitude (red vertical line).

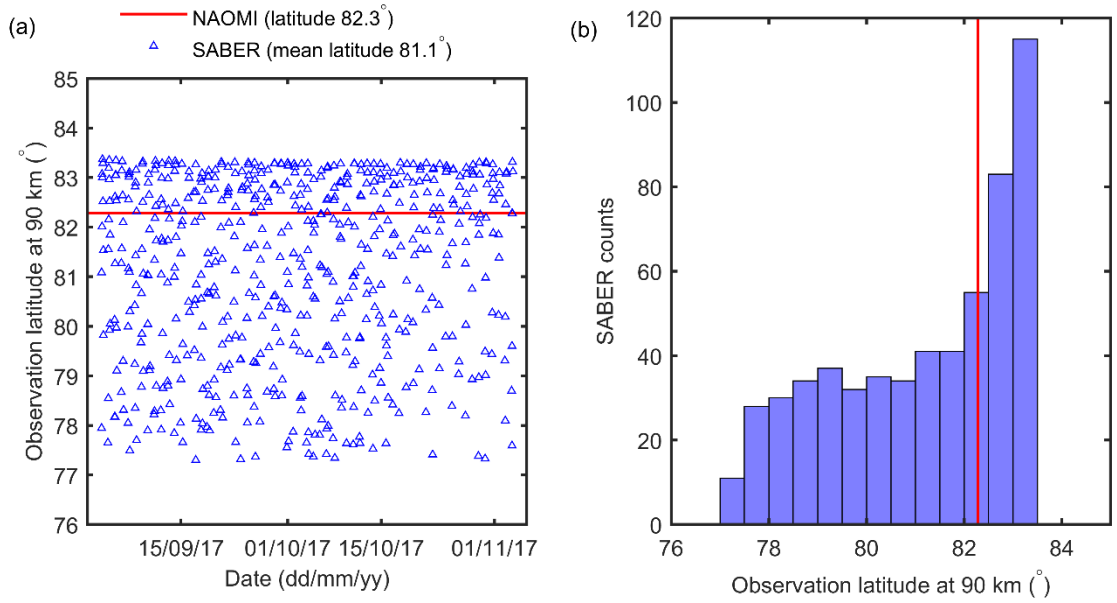

Figure ACA1-7: Latitudes at altitude 90 km for NAOMI and SABER observations during 2017 autumn twilight (2 September – 3 November 2017, 75° ≤ SZA at altitude 90 km ≤ 110°) conditions: (**a**) time series of observation latitudes and **(b)** histogram of SABER observation latitudes compared with NAOMI observation latitude (red vertical line).

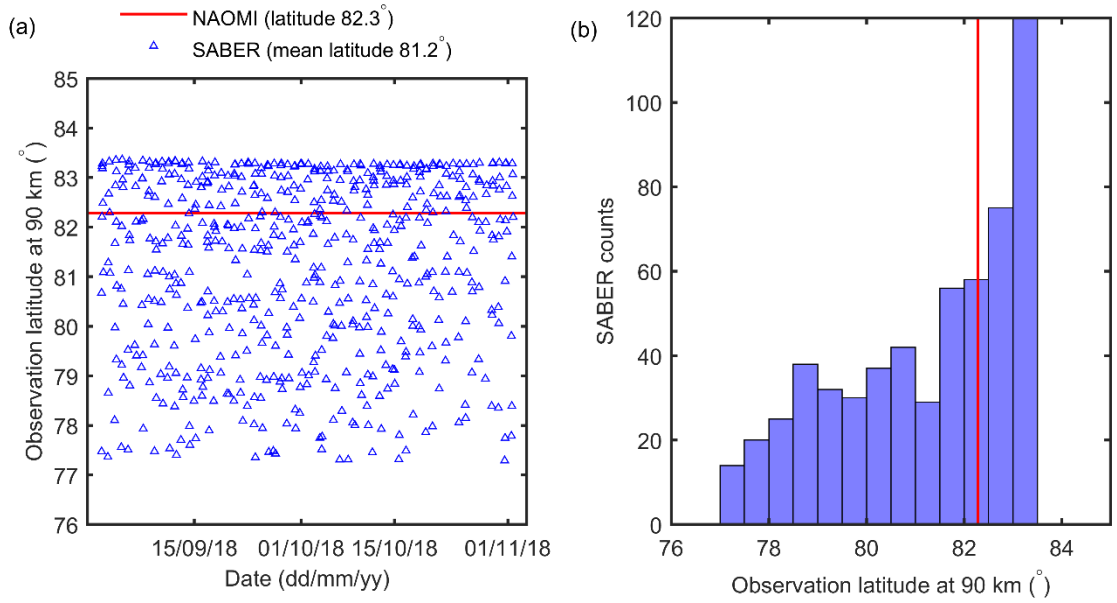

Figure ACA1-8: Latitudes at altitude 90 km for NAOMI and SABER observations during 2018 autumn twilight (31 August – 1 November 2018, 75° ≤ SZA at altitude 90 km ≤ 110°) conditions: (**a**) time series of observation latitudes and **(b)** histogram of SABER observation latitudes compared with NAOMI observation latitude (red vertical line).

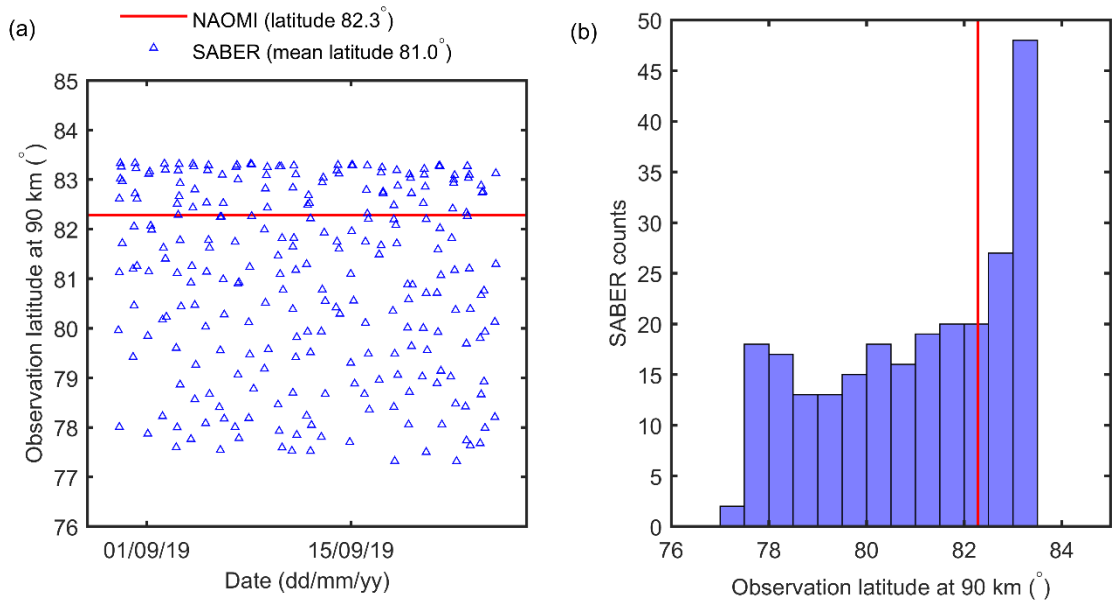

Figure ACA1-9: Latitudes at altitude 90 km for NAOMI and SABER observations during 2019 autumn twilight (29 August – 25 September 2019, 75° ≤ SZA at altitude 90 km ≤ 110°) conditions: (**a**) time series of observation latitudes and **(b)** histogram of SABER observation latitudes compared with NAOMI observation latitude (red vertical line).

Appendix ACA2 – Plots of NAOMI and SABER observation solar zenith angle

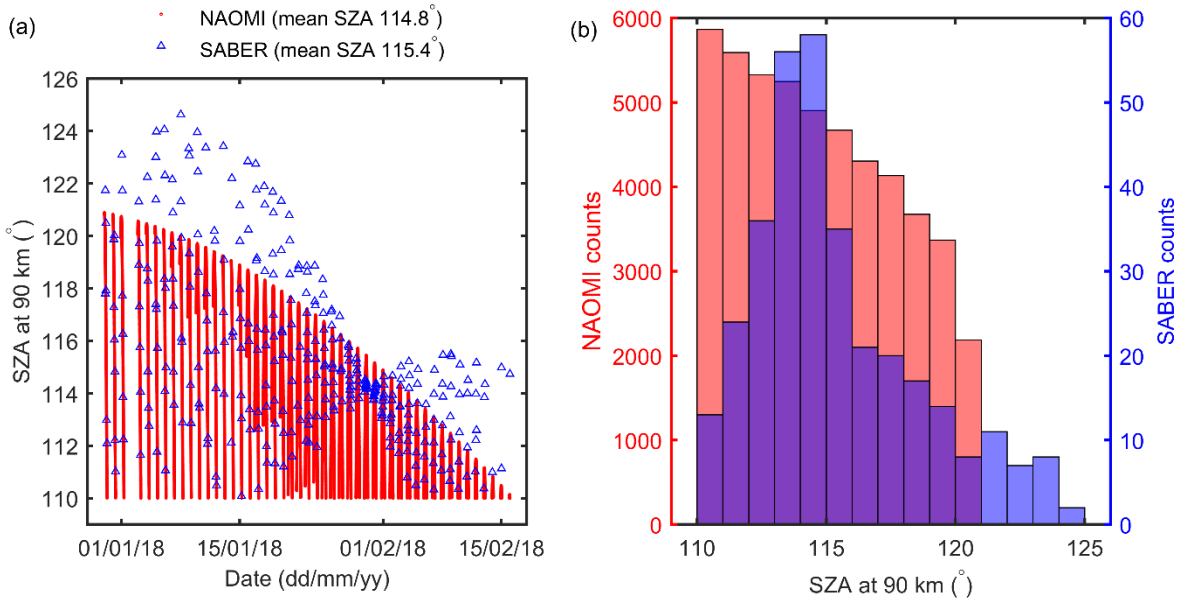

Figure ACA2-1: Solar zenith angles (SZAs) at altitude 90 km for NAOMI and SABER observations during 2017–18 winter night-time (29 December 2017 – 16 February 2018, SZA at altitude 90 km > 110°) conditions: (**a**) time series and **(b)** histograms of NAOMI and SABER SZAs.

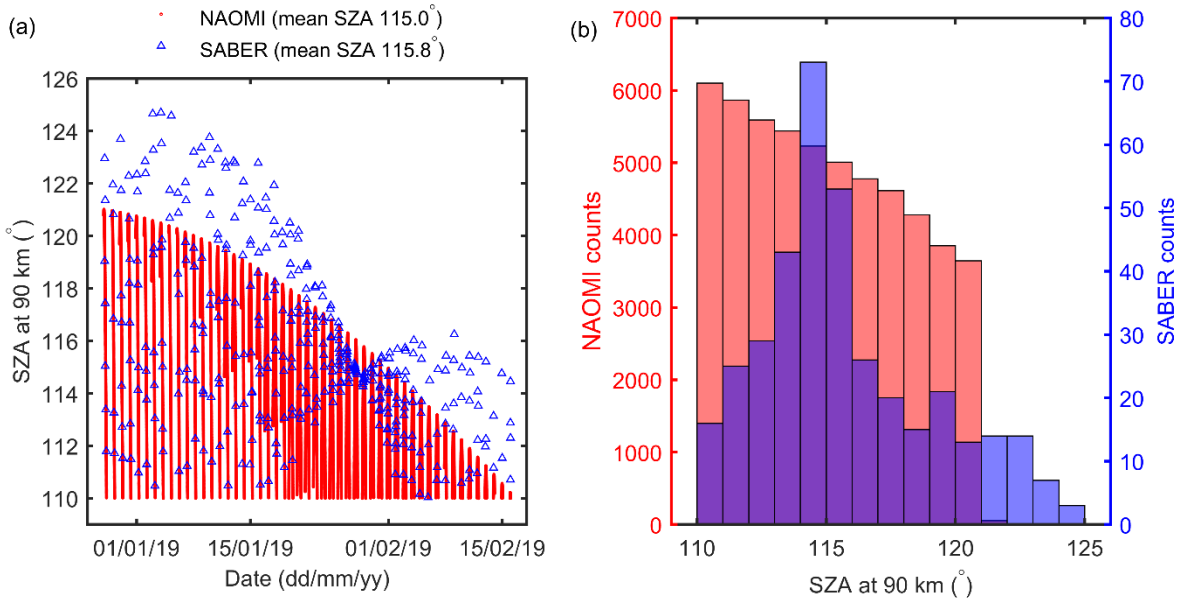

Figure ACA2-2: Solar zenith angles (SZAs) at altitude 90 km for NAOMI and SABER observations during 2018–19 winter night-time (27 December 2018 – 16 February 2019, SZA at altitude 90 km > 110°) conditions: (**a**) time series and **(b)** histograms of NAOMI and SABER SZAs.

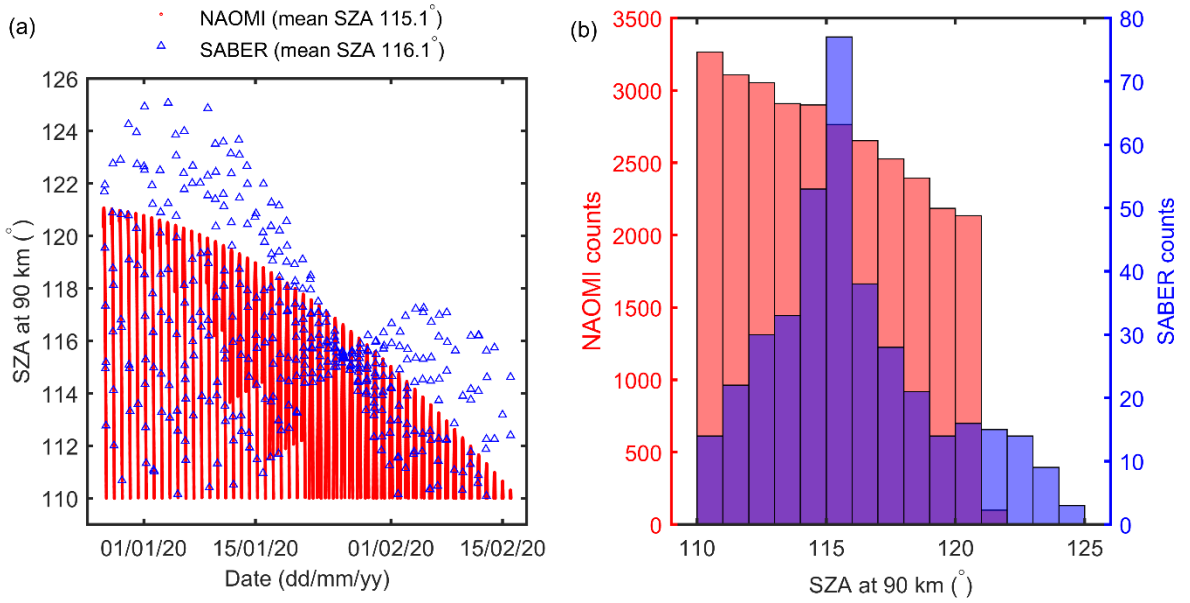

Figure ACA2-3: Solar zenith angles (SZAs) at altitude 90 km for NAOMI and SABER observations during 2019–20 winter night-time (26 December 2019 – 16 February 2020, SZA at altitude 90 km > 110°) conditions: (**a**) time series and **(b)** histograms of NAOMI and SABER SZAs.

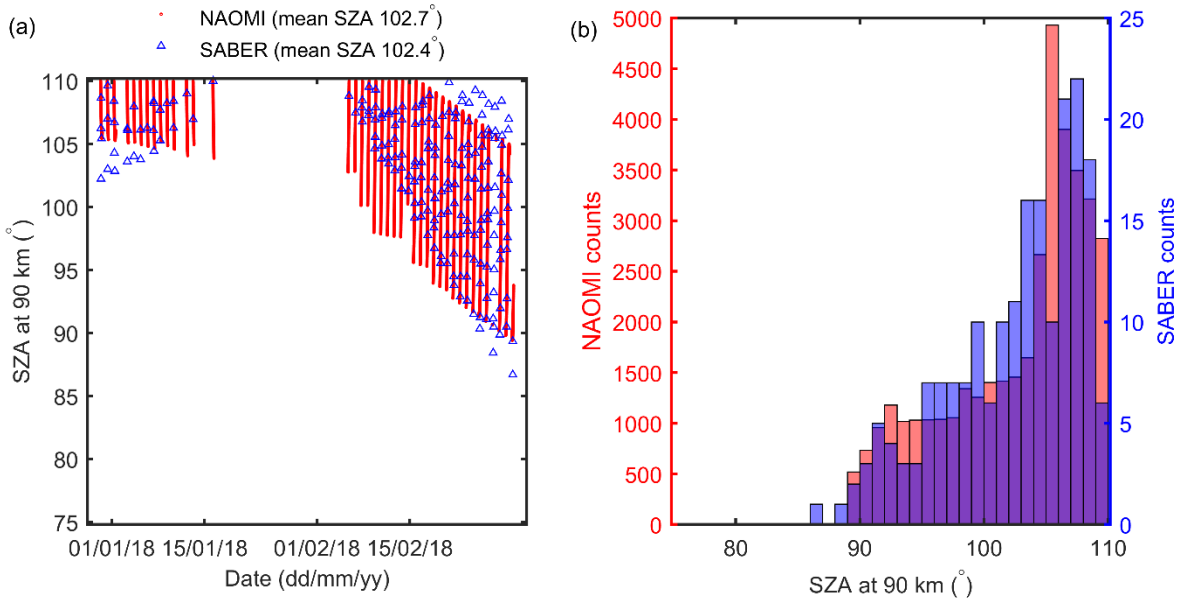

Figure ACA2-4: Solar zenith angles (SZAs) at altitude 90 km for NAOMI and SABER observations during 2017–18 winter twilight (30 December 2017 – 2 March 2018, 75° ≤ SZA at altitude 90 km ≤ 110°) conditions: (**a**) time series and **(b)** histograms of NAOMI and SABER SZAs.

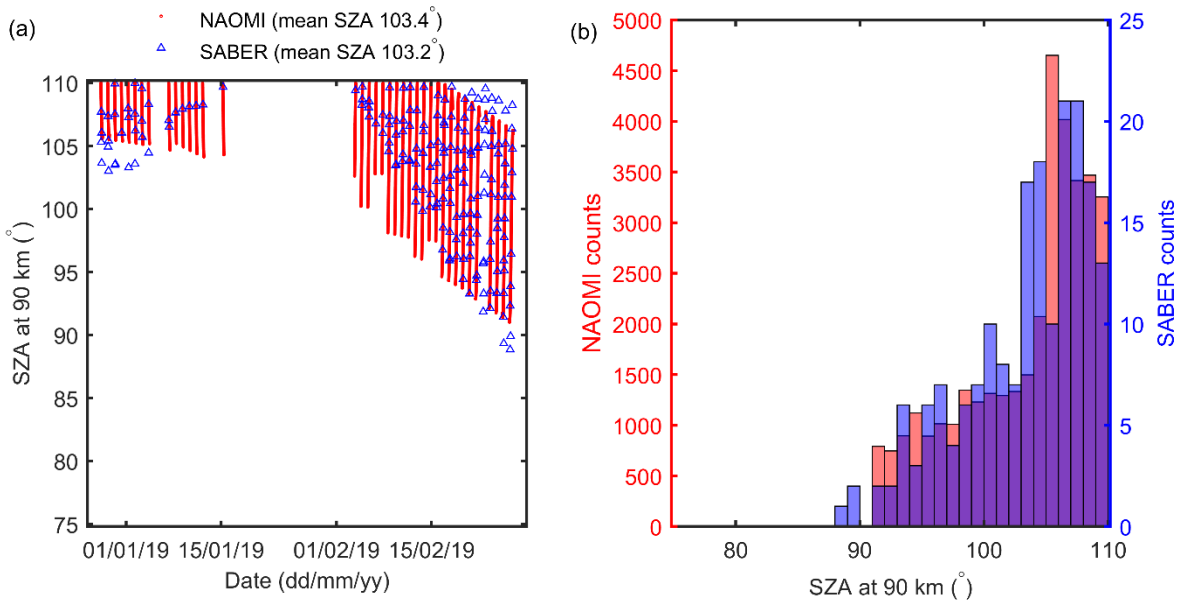

Figure ACA2-5: Solar zenith angles (SZAs) at altitude 90 km for NAOMI and SABER observations during 2018–19 winter twilight (28 December 2018 – 27 February 2019, 75° ≤ SZA at altitude 90 km ≤ 110°) conditions: (**a**) time series and **(b)** histograms of NAOMI and SABER SZAs.

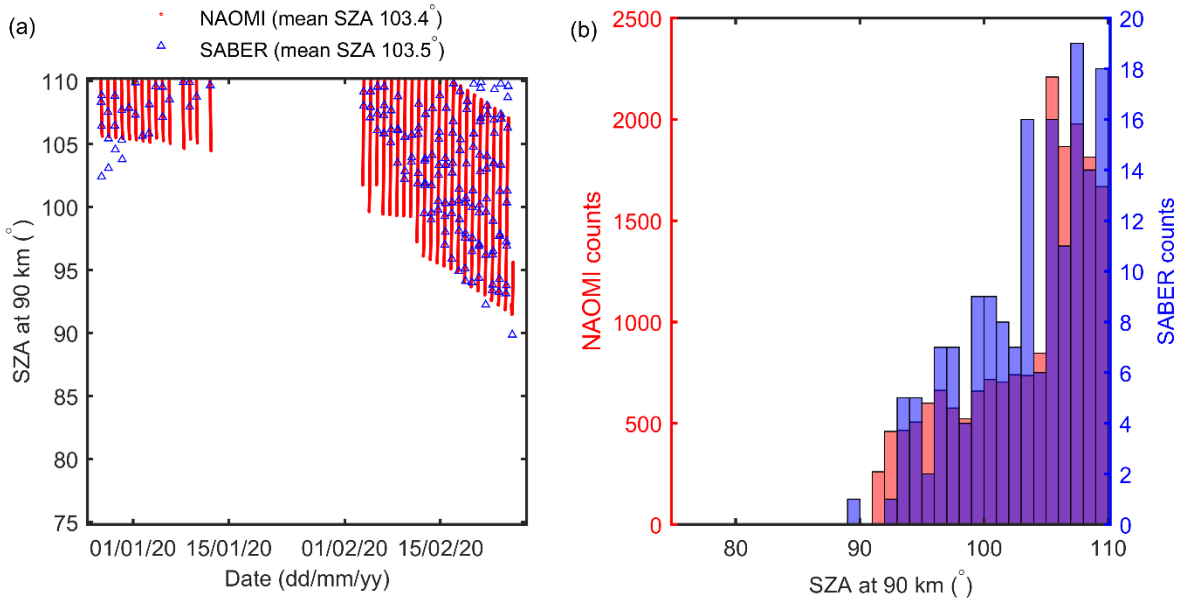

Figure ACA2-6: Solar zenith angles (SZAs) at altitude 90 km for NAOMI and SABER observations during 2019–20 winter twilight (27 December 2019 – 25 February 2020, 75° ≤ SZA at altitude 90 km ≤ 110°) conditions: (**a**) time series and **(b)** histograms of NAOMI and SABER SZAs.

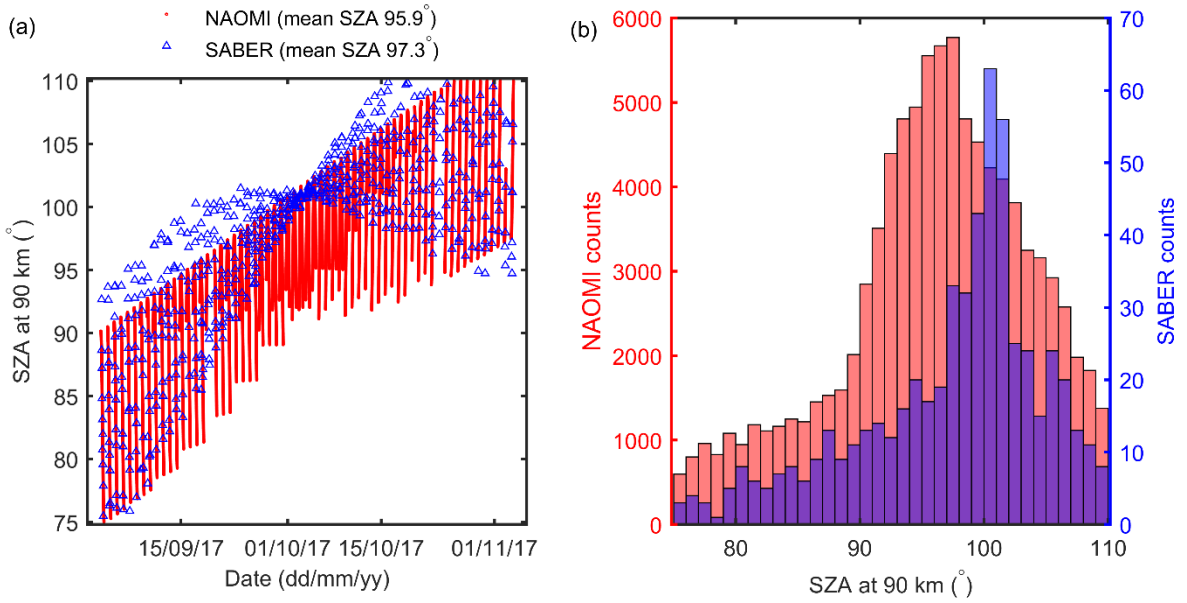

Figure ACA2-7: Solar zenith angles (SZAs) at altitude 90 km for NAOMI and SABER observations during 2017 autumn twilight (2 September – 3 November 2017, 75° ≤ SZA at altitude 90 km ≤ 110°) conditions: (**a**) time series and **(b)** histograms of NAOMI and SABER SZAs.

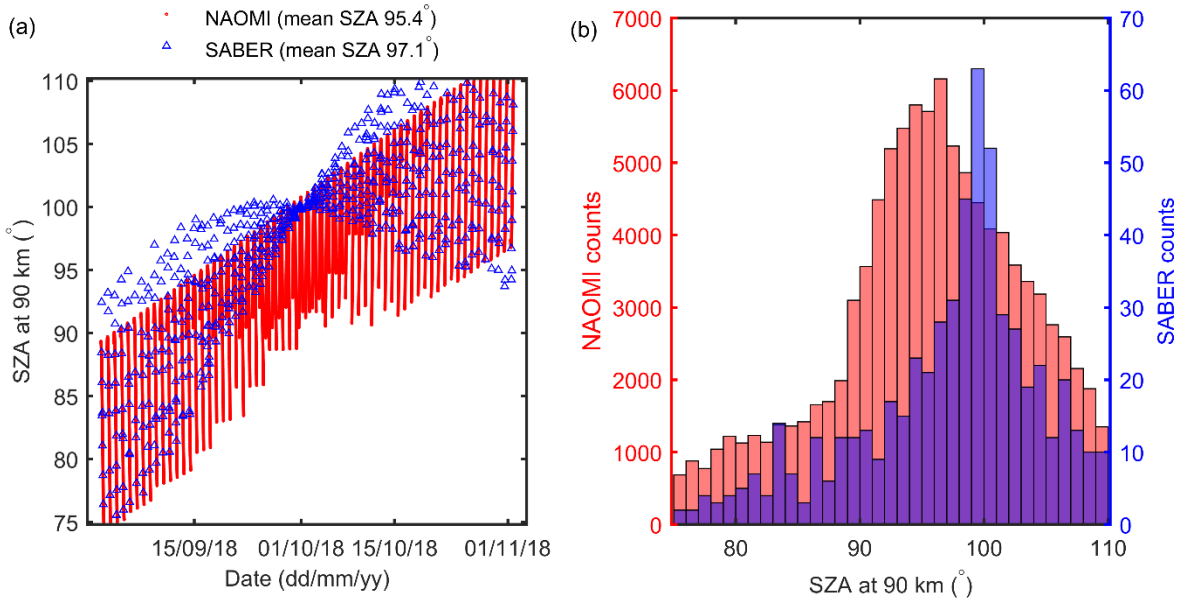

Figure ACA2-8: Solar zenith angles (SZAs) at altitude 90 km for NAOMI and SABER observations during 2018 autumn twilight (31 August – 1 November 2018, 75° ≤ SZA at altitude 90 km ≤ 110°) conditions: (**a**) time series and **(b)** histograms of NAOMI and SABER SZAs.

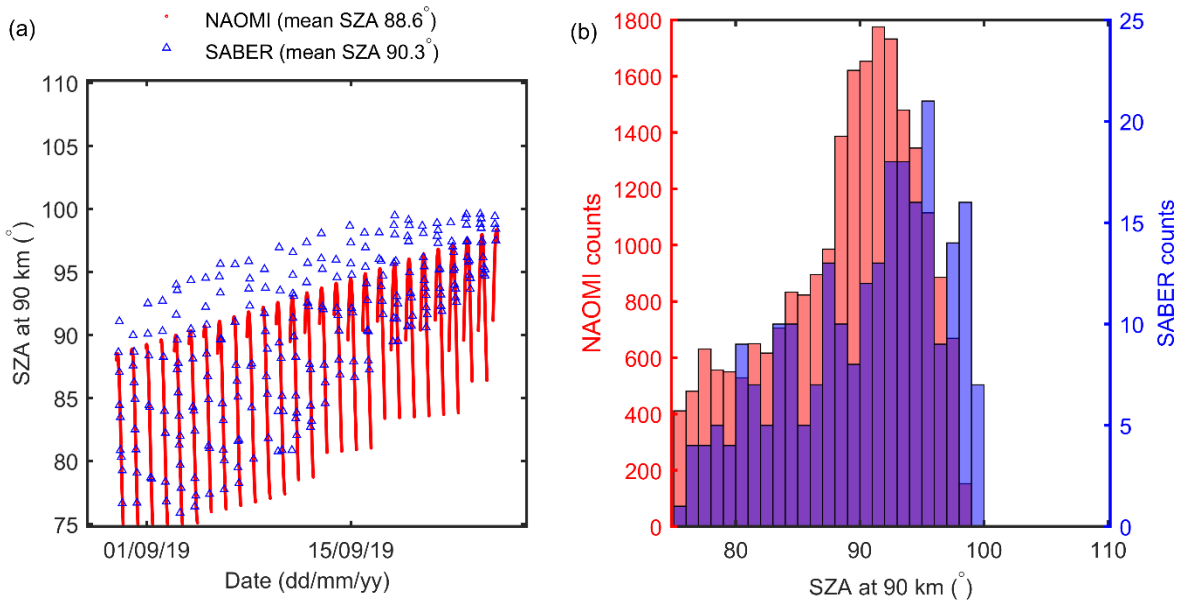

Figure ACA2-9: Solar zenith angles (SZAs) at altitude 90 km for NAOMI and SABER observations during 2019 autumn twilight (29 August – 25 September 2019, 75° ≤ SZA at altitude 90 km ≤ 110°) conditions: (**a**) time series and **(b)** histograms of NAOMI and SABER SZAs.

Appendix ACA3 – Plots of NAOMI and SABER observation times

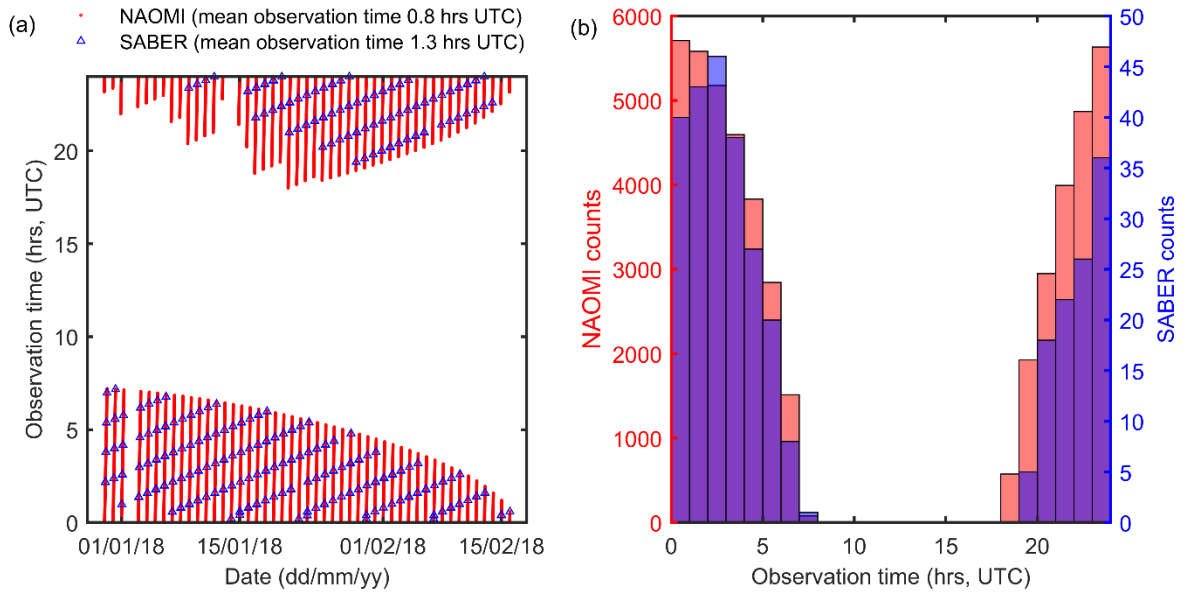

Figure ACA3-1: Observation times for NAOMI and SABER observations during 2017–18 winter night-time (29 December 2017 – 16 February 2018, SZA at altitude 90 km > 110°) conditions: (**a**) time series and **(b)** histograms of NAOMI and SABER observation times.

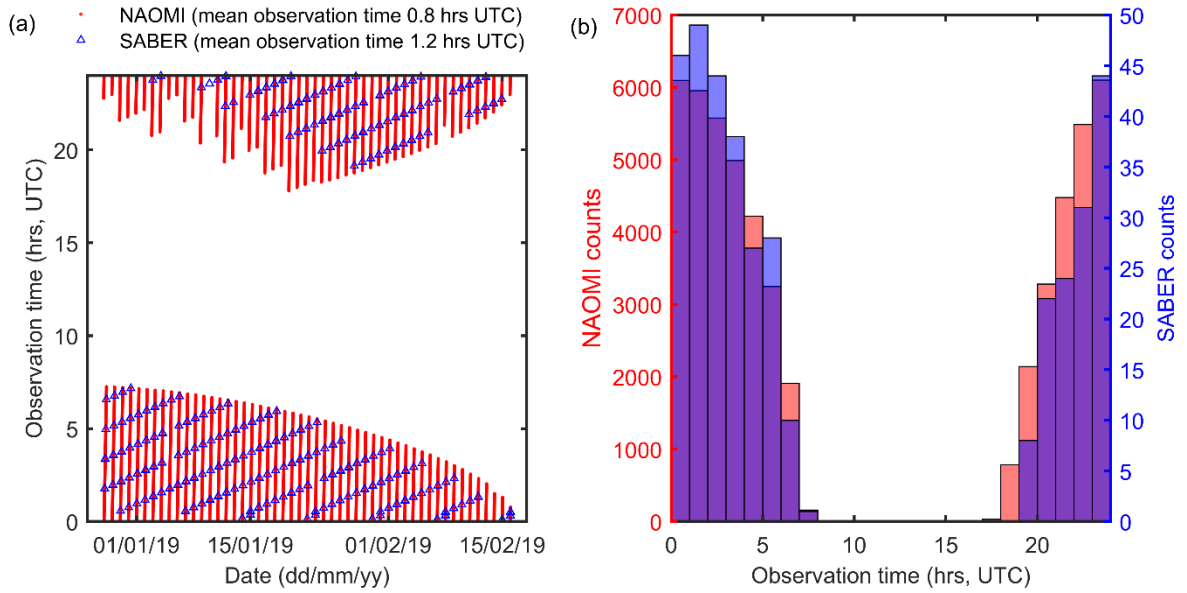

Figure ACA3-2: Observation times for NAOMI and SABER observations during 2018–19 winter night-time (27 December 2018 – 16 February 2019, SZA at altitude 90 km > 110°) conditions: (**a**) time series and **(b)** histograms of NAOMI and SABER observation times.

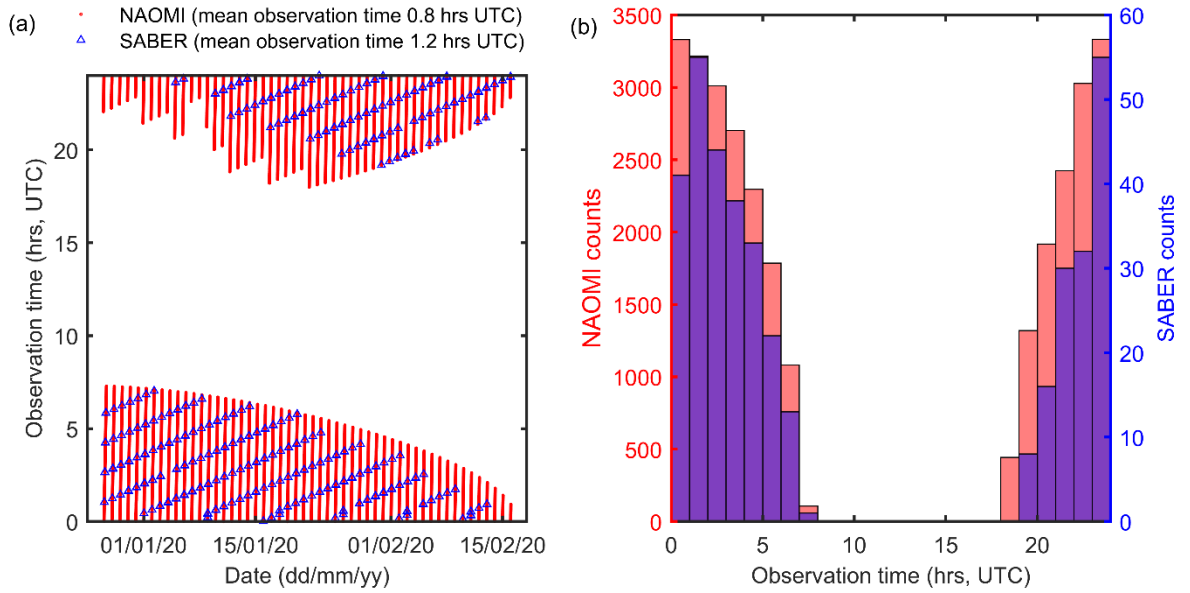

Figure ACA3-3: Observation times for NAOMI and SABER observations during 2019–20 winter night-time (26 December 2019 – 16 February 2020, SZA at altitude 90 km > 110°) conditions: (**a**) time series and **(b)** histograms of NAOMI and SABER observation times.

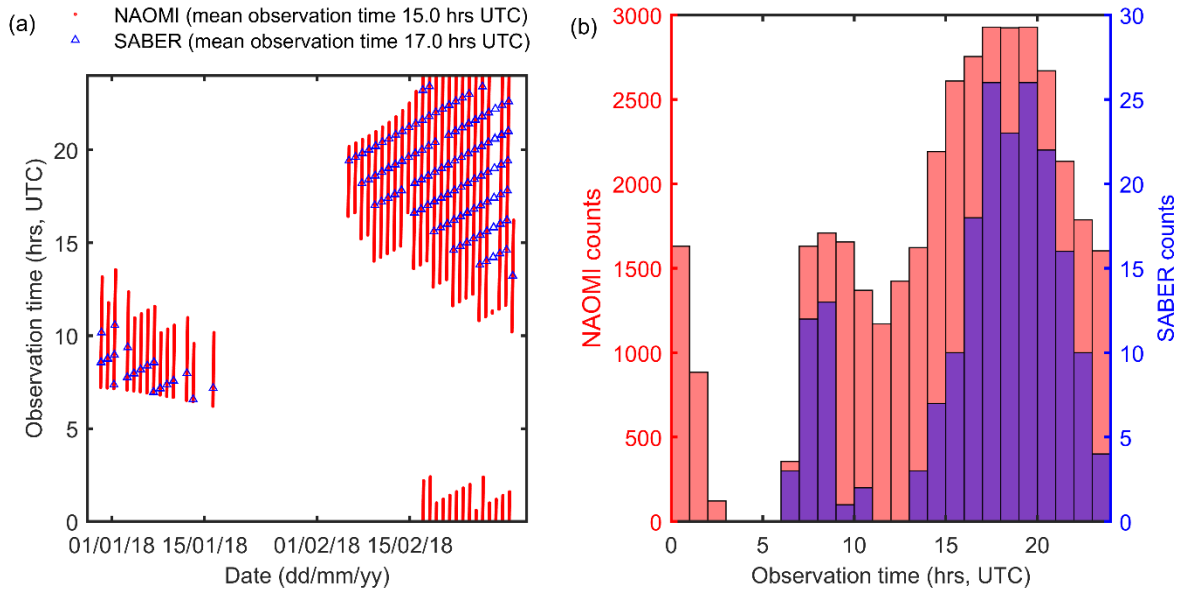

Figure ACA3-4: Observation times for NAOMI and SABER observations during 2017–18 winter twilight (30 December 2017 – 2 March 2018, 75° ≤ SZA at altitude 90 km ≤ 110°) conditions: (**a**) time series and **(b)** histograms of NAOMI and SABER observation times.

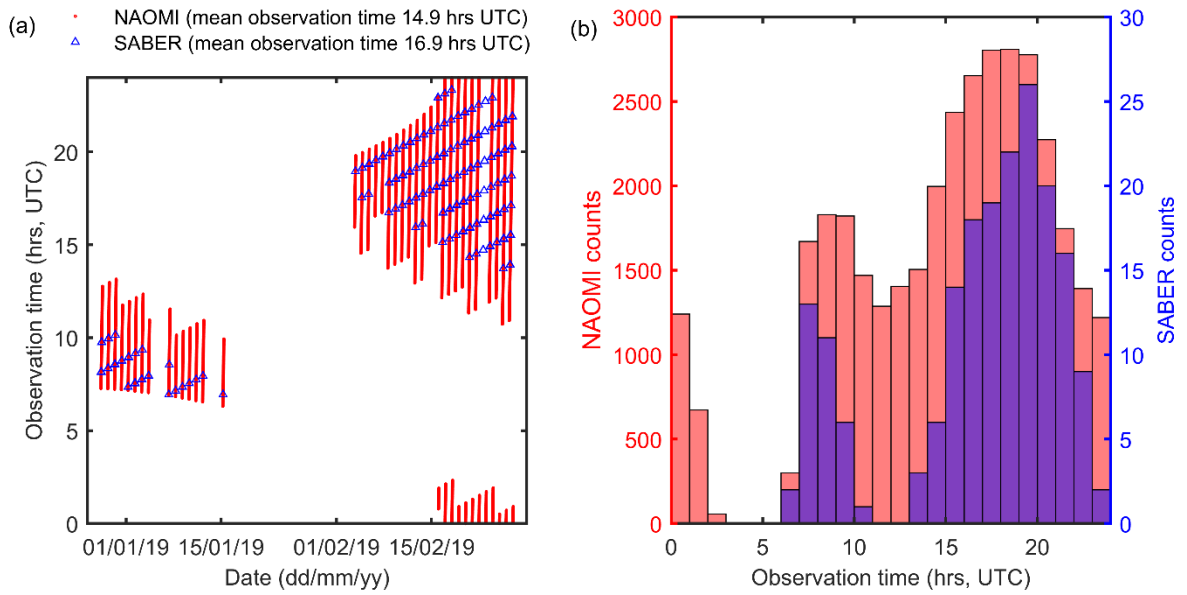

Figure ACA3-5: Observation times for NAOMI and SABER observations during 2018–19 winter twilight (28 December 2018 – 27 February 2019, 75° ≤ SZA at altitude 90 km ≤ 110°) conditions: (**a**) time series and **(b)** histograms of NAOMI and SABER observation times.

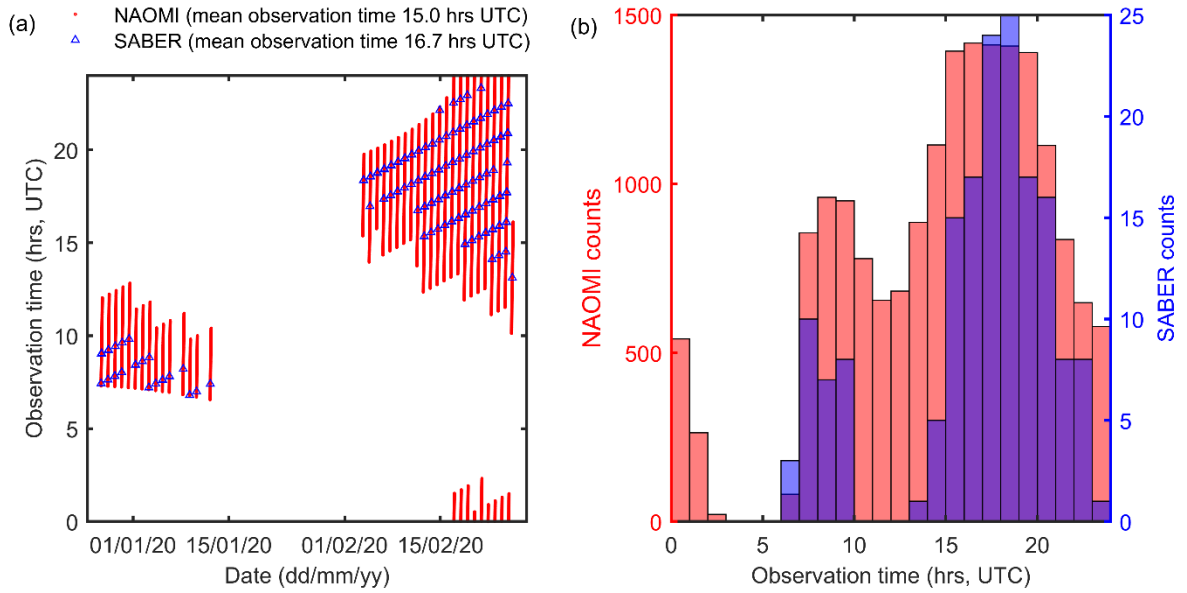

Figure ACA3-6: Observation times for NAOMI and SABER observations during 2019–20 winter twilight (27 December 2019 – 25 February 2020, 75° ≤ SZA at altitude 90 km ≤ 110°) conditions: (**a**) time series and **(b)** histograms of NAOMI and SABER observation times.

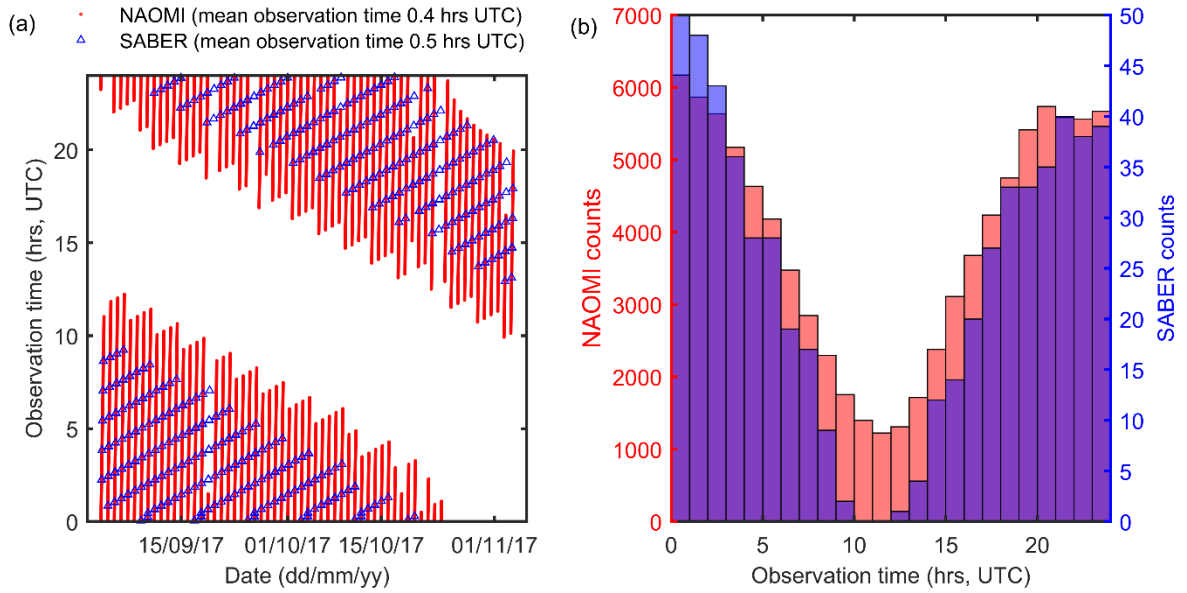

Figure ACA3-7: Observation times for NAOMI and SABER observations during 2017 autumn twilight (2 September – 3 November 2017, 75° ≤ SZA at altitude 90 km ≤ 110°) conditions: (**a**) time series and **(b)** histograms of NAOMI and SABER observation times.

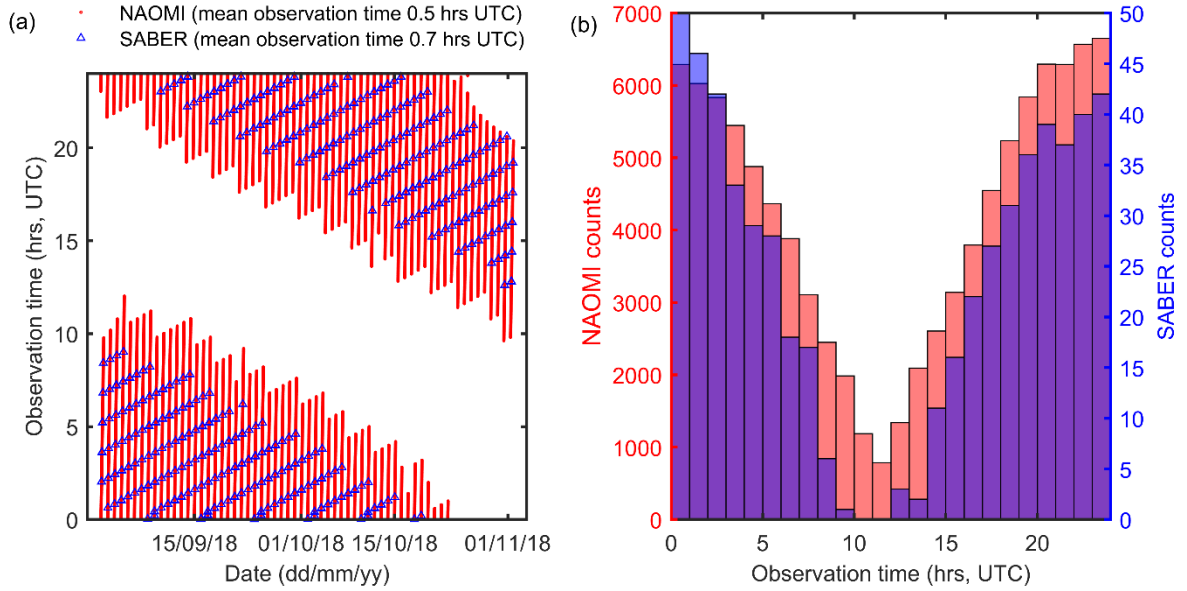

Figure ACA3-8: Observation times for NAOMI and SABER observations during 2018 autumn twilight (31 August – 1 November 2018, 75° ≤ SZA at altitude 90 km ≤ 110°) conditions: (**a**) time series and **(b)** histograms of NAOMI and SABER observation times.

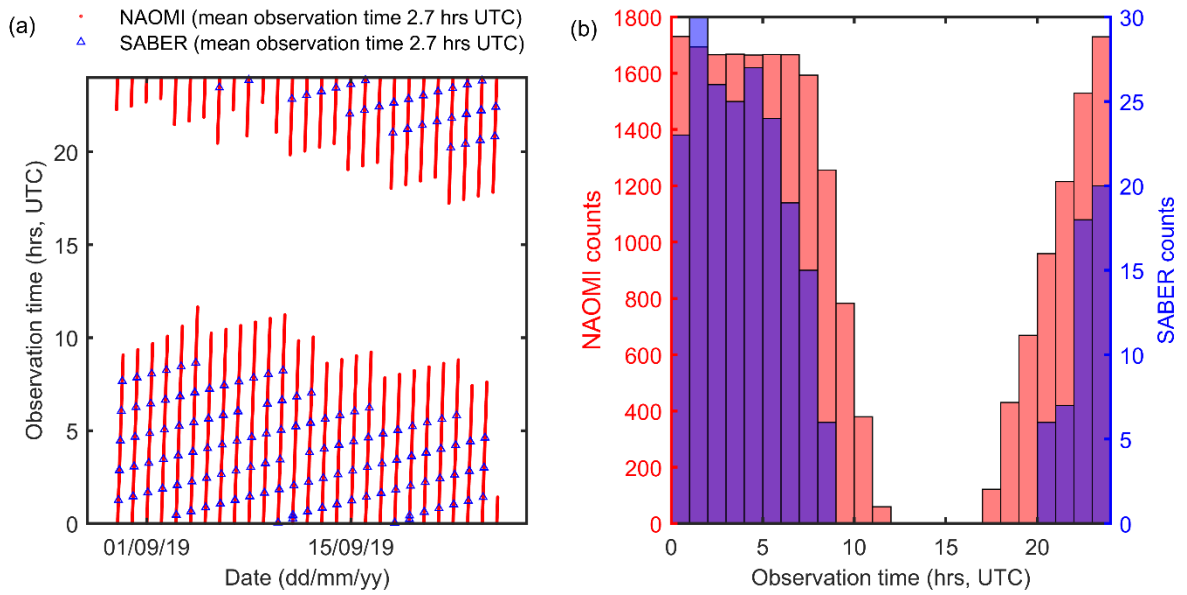

Figure ACA3-9: Observation times for NAOMI and SABER observations during 2019 autumn twilight (29 August – 25 September 2019, 75° ≤ SZA at altitude 90 km ≤ 110°) conditions: (**a**) time series and **(b)** histograms of NAOMI and SABER observation times.